Biophysical Chemistry 141 (2009) 169–174

Contents lists available at ScienceDirect

Biophysical Chemistry

journal homepage: http://www.elsevier.com/locate/biophyschem

Self assembly of a model amphiphilic phenylalanine peptide/polyethylene glycol block copolymer in aqueous solution

Valeria Castelletto, Ian W. Hamley *

Dept. of Chemistry, University of Reading, Reading RG6 6AD, UK

ARTICLE INFO

Article history:
Received 13 December 2008
Received in revised form 23 January 2009
Accepted 23 January 2009
Available online 3 February 2009

Keywords:
Peptide copolymers
Self-assembly
Beta sheets
Fibrils

ABSTRACT

There has been great interest recently in peptide amphiphiles and block copolymers containing biomimetic peptide sequences due to applications in bionanotechnology. We investigate the self-assembly of the peptide-PEG amphiphile FFFF-PEG5000 containing the hydrophobic sequence of four phenylalanine residues conjugated to PEG of molar mass 5000. This serves as a simple model peptide amphiphile. At very low concentration, association of hydrophobic aromatic phenylalanine residues occurs, as revealed by circular dichroism and UV/vis fluorescence experiments. A critical aggregation concentration associated with the formation of hydrophobic domains is determined through pyrene fluorescence assays. At higher concentration, defined β-sheets develop as revealed by FTIR spectroscopy and X-ray diffraction. Transmission electron microscopy reveals self-assembled straight fibril structures. These are much shorter than those observed for amyloid peptides, the finite length may be set by the end cap energy due to the hydrophobicity of phenylalanine. The combination of these techniques points to different aggregation processes depending on concentration. Hydrophobic association into irregular aggregates occurs at low concentration, well-developed β-sheets only developing at higher concentration. Drying of FFFF-PEG5000 solutions leads to crystallization of PEG, as confirmed by polarized optical microscopy (POM), FTIR and X-ray diffraction (XRD). PEG crystallization does not disrupt local β-sheet structure (as indicated by FTIR and XRD). However on longer lengthscales the β-sheet fibrillar structure is perturbed because spherulites from PEG crystallization are observed by POM.

1. Introduction

The world of amphiphiles is a rich and diverse one [1,2]. Conventional synthetic surfactants are the basis of detergents. Lipids are natural amphiphiles whose main role is in structuring the cell membrane. Peptide-containing amphiphiles have been the focus of recent attention because the specificity of peptide interactions (eg. targeted binding to proteins) can potentially be combined with amphiphilic properties such as self-assembly into micelles to create novel materials with hybrid properties [3–5]. There are three broad classes of peptide amphiphile — those with hydrophilic peptides attached to hydrophobic chains [6–11], the inverse case of hydrophobic peptides attached to hydrophilic chains [12–17] and thirdly surfactant-like peptides comprising connected sequences of hydrophobic and hydrophilic amino acids [9,18–20]. The former category mainly comprises peptides attached to alkyl chains of which dodecyl to octadecyl chains are of most interest in terms of amphiphilicity [11,21]. The second class includes peptides conjugated to poly(ethylene glycol) (PEG).

We have recently begun a programme to investigate the self-assembly of peptide amphiphiles comprising peptides based on a fragment of the amyloid beta peptide, Aβ(16–20), i.e. KLVFF, conjugated to PEG including peptide amphiphiles such as FFKLVFF-PEG (PEG $M_n = 3300$). KLVFF has been identified as a minimal key sequence in the formation of amyloid fibrils by the full Aβ peptide [22,23]. FFKLVFF contains the peptide sequence FFKLVFF, which is Aβ(16–20) extended by two phenylalanine residues. FFKLVFF is highly hydrophobic and does not dissolve in water (it does fibrillise in methanol [24]). However, conjugation to PEG leads to an amphiphilic molecule which forms self-assembled fibrillar structures in dilute aqueous solution, and nematic and hexagonal columnar liquid crystal phases at higher concentration [17,25,26].

In an effort to understand the role of different intermolecular interactions in the self-assembly process we have investigated the peptide amphiphile FFFF-PEG (with PEG $M_n = 5000$ approximately) in which the peptide comprises purely hydrophobic phenylalanine residues. There are no charged or polar residues in the FFFF in contrast to FFKLVFF-PEG studied by us recently, so FFFF-PEG constitutes a model peptide amphiphile based around a short hydrophobic peptide moiety. It should be noted that the end groups of this conjugate are charged (Scheme 1) so electrostatic interactions

* Corresponding author. Also at Diamond Light Source, Harwell Science and Innovation Campus, Chilton, Didcot, Oxfordshire OX11 0DE, UK.
E-mail address: I.W.Hamley@reading.ac.uk (I.W. Hamley).

0301-4622/$ – see front matter © 2009 Elsevier B.V. All rights reserved.
doi:10.1016/j.bpc.2009.01.008

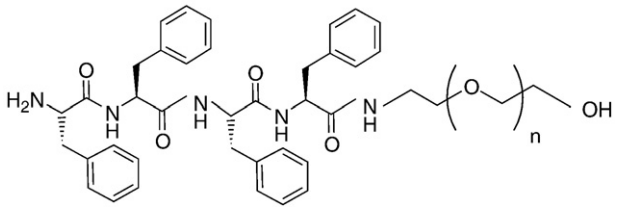

Scheme 1. Structure of FFFF-PEG, n = 100 approximately.

may influence self-assembly, although the peptide moiety itself is uncharged.

In pioneering work, Gazit and coworkers have shown that diphenylalanine forms nanotubes in aqueous solution, and that this can be used for bionanotechnology applications such as the fabrication of metal nanowires [27]. The original motivation for studying phenylalanine-based peptides was the observation of the importance of these residues in amyloid formation [28,29]. The use of Fmoc-dipeptides to form hydrogels for three-dimensional cell culture has also been explored [30,31]. However, to our knowledge there has been no prior work on PEGylated phenylalanine peptides. Conjugation of PEG is expected to confer amphiphilic properties, and these may be useful in the preparation of self-assembled materials. For instance, PEG has well-known properties as a steric stabiliser, preventing or hindering uptake, or facilitating slow release, and is approved for medical applications. The focus of our initial work presented here is on the self-assembly of a model FFFF-PEG peptide.

2. Experimental section

2.1. Materials

The PEGylated conjugate FFFF-PEG (Scheme 1) was synthesized by Rapp polymers GmbH using solid phase peptide synthesis methods. PEGylated TentaGel PAP resin was used, and the peptide was assembled from the C-terminus towards the N-terminus, and was attached to the solid support at the C-terminal by the α-carbonyl group of the amino acid. The crude peptides were characterized by reverse phase high performance liquid chromatography (RP-HPLC; Grom Saphir 200, C18 5 μm column). A mobile phase of water with 0.1% TFA and acetonitrile with 0.08% TFA was used. Sample elution was monitored using a UV/vis detector operating at 220 nm. MALDI-TOF (Ultraflex, Bruker with matrix Universalmatrix Fluka) was used to confirm $M_n = 5680$ g mol^{-1}, consistent with addition of tetraphenylalanine to the precursor PEG ($M_n = 4850$ g mol^{-1}, MALDI-TOF). Schulz–Zimm fitting of the molecular weight distribution indicates $M_w/M_n < 1.05$.

2.2. Circular dichroism (CD)

Spectra were recorded on a Chirascan spectropolarimeter (Applied Photophysics, UK). CD for solutions was performed using samples dissolved in water (0.04, 1 and 4.5 wt.%) and loaded into a 0.1 mm quartz cover slip cuvette. CD experiments were also performed on dried films from the same solutions, obtained by drying a few drops of the solution on a cover slip. Spectra are presented with absorbance $A < 2$ at any measured point with a 0.5 nm step, 1 nm bandwidth and 1 s collection time per step at 20 °C, taking five averages.

2.3. Fluorescence spectroscopy

Spectra were recorded on a Perkin Elementar Luminescence spectrometer LS50B with samples in a 1.0 cm quartz cuvette. Spectra were measured for FFFF-PEG in water (0.01 wt.%). The spectra were recorded from 285 to 490 nm using an excitation wavelength $\lambda_{ex} = 265$ nm. The same spectrometer was used for the thioflavin T (ThT) and pyrene assays described below. For all the fluorescence studies the spectra were recorded taking five averages at room temperature and the water background was subtracted.

ThT assays were performed using a 1.6×10^{-3} wt.% ThT solution. Samples containing 0, 0.006, 0.023 and 0.1 wt.% FFFF-PEG in this ThT solution were studied. The spectra of 0.01 and 0.05 wt.% FFFF-PEG solutions in water were used as reference. All spectra were measured from 460 to 700 nm, using $\lambda_{ex} = 440$ nm.

Pyrene fluorescence assays were made using a sample containing only pyrene (3×10^{-6} wt.%), and a set of samples containing (0.0064–0.4) wt.% FFFF-PEG with 3×10^{-6} wt.% pyrene. All spectra were measured from 360 to 460 nm, using $\lambda_{ex} = 339$ nm.

2.4. Fourier Transform Infra-red (FTIR) spectroscopy

Spectra were measured on a Nicolet Nexus spectrometer with DTGS detector. Sample solutions in D_2O (2.5–20 wt.%) were sandwiched between two CaF_2 plate windows (spacer 0.006 mm) and a solid film of dry peptide was deposited on one CaF_2 plate by drying a solution. Spectra were scanned 28 times over the range of 4000–400 cm^{-1}.

2.5. Transmission electron microscopy (TEM)

Experiments were performed using a Philips CM20 transmission electron microscope operated at 80 kV while HR-TEM was done using a JEOL microscope operated at 100 kV. A droplet of 1 wt.% FFFF-PEG solution was placed on a Cu grid coated with a carbon film (Agar Scientific, UK), stained with uranyl acetate (1 wt.%) (Agar Scientific, UK) and dried.

2.6. X-ray diffraction (XRD)

Diffraction patterns were obtained for stalks prepared by drying filaments of the peptide. An aqueous solution of the peptide (17 wt.%) was suspended between the ends of a wax-coated capillary and dried. The stalk was mounted (vertically) onto the four axis goniometer of a R-AXIS IV++ X-ray diffractometer (Rigaku) equipped with a rotating anode generator. The XRD data was collected using a Saturn 992 CCD camera.

2.7. Polarized optical microscopy (POM)

Microscopy experiments were performed by placing the sample between crossed polarizers in an Olympus BX41 polarized microscope. A few drops of 10 wt.% FFFF-PEG were placed on a glass slide and left to dry before capturing the image with a Canon G2 digital camera.

3. Solution self-assembly

The secondary structure of PEGylated peptides was assessed using circular dichroism and UV absorption/fluorescence spectroscopy for dilute solutions and FTIR spectroscopy for more concentrated solutions.

Fig. 1 shows CD spectra for FFFF-PEG at several concentrations. There is a pronounced positive maximum at 220 nm. This can be assigned to n–π* transitions resulting from aromatic stacking interactions of the phenylalanine residues. Similar features were noted for FFKLVFF [24] and FFKLVFF-PEG [17]. This indicates that PEG does not substantially modulate this signal. In dried films, the CD spectra show a negative maximum at 216 nm, consistent with well-developed β-sheet structures. This feature becomes more pronounced as the concentration of solution from which the film was dried was increased.

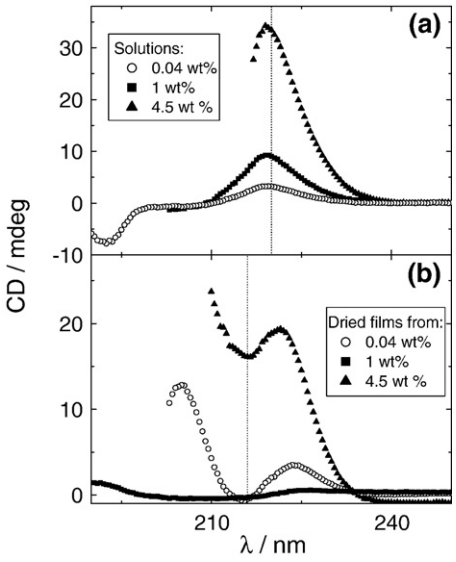

Fig. 1. Circular dichroism (CD) spectra, measured for FFFF-PEG (a) in aqueous solutions and (b) for films dried from the same solutions.

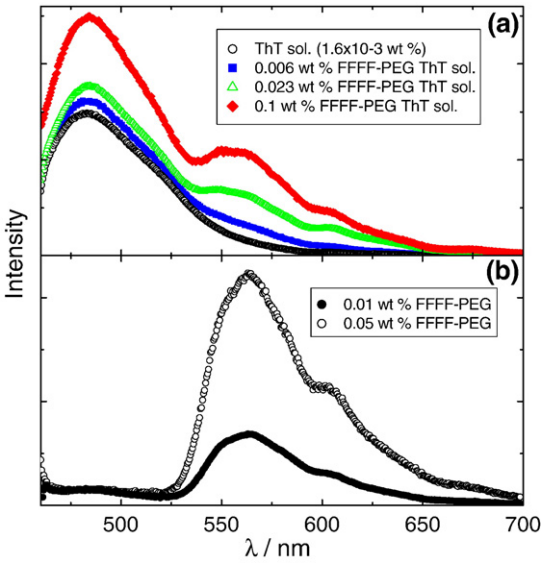

Fig. 3. Fluorescence spectra of FFFF-PEG with (a) and without (b) ThT, including ThT control spectrum (concentrations indicated, $\lambda_{ex}=440$ nm). The error bars, calculated from repeat measurements over 2 days, fall within the limits of the data points.

Fluorescence spectroscopy confirmed the role of aromatic stacking interactions between phenylalanine residues in the self-assembly process. Fig. 2 presents a spectrum for a 0.01 wt.% aqueous solution of FFFF-PEG. The peak at 310 nm is associated with π–π stacking interactions as discussed elsewhere [24,32]. Interestingly, despite the presence of PEG, the conjugate exhibited binding of thioflavin T (ThT), a dye staining method commonly used as a diagnostic for amyloid formation [33,34]. Fig. 3 shows the increase in the 480 nm peak intensity in the fluorescence spectrum due to increased binding of ThT and FFFF-PEG as the peptide conjugate concentration is increased. An additional feature of note in these spectra is the peak at around 560 nm due to the peptide alone, also observed in the presence of ThT and increasing in intensity with conjugate concentration. This peak is absent for ThT on its own. This "green fluorescence" peak was also observed for FFKLVFF stained with congo red [24]. A similar peak has been reported for other amphiphilic molecules comprising aromatic moieties conjugated to PEG chains [35]. A detailed explanation of its origin is still lacking. Ulijn and coworkers have ascribed strongly red shifted maxima (broad peak at 460 nm, red shifted from main peak at 320 nm) in fluorescence emission spectra to the formation of so-called J-aggregates which arise from stacking of aromatic moieties (phenylalanine in their case) [31]. In our case, we are not sure if the 560 nm excimer peak can be ascribed to this phenomenon, since the red shift would be much greater.

FTIR (Fig.4) was used to probe peptide secondary structure in solution but also contained a series of peaks from crystalline poly (ethylene glycol) in the solid state, as discussed in the following section. We focus here on the amide I region. In solution, the spectrum for the 2.5 wt.% solution contains a single maximum at 1660 cm^{-1}, probably due to turn or bend structures [36,37]. On increasing concentration above 5 wt.%, a splitting with maxima at around 1646 cm^{-1} and 1670 cm^{-1} is observed. The peak at 1646 cm^{-1} is probably due to random coil structures or unordered structures [36–39], the shoulder at approximately 1670 cm^{-1} may be associated with an antiparallel β-sheet structure [37], as supported by its correlation to the peak

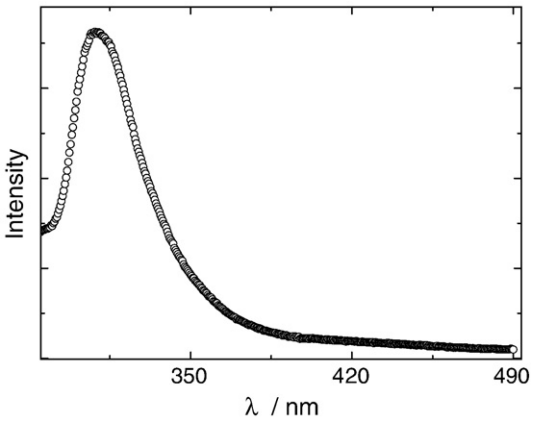

Fig. 2. Fluorescence spectrum of FFFF-PEG in water (0.01 wt.%, $\lambda_{ex}=265$ nm).

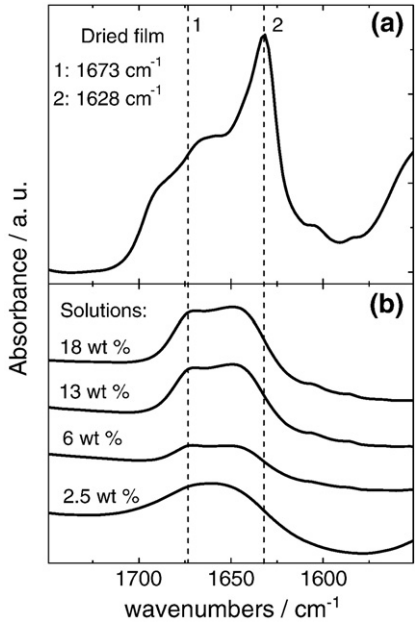

Fig. 4. FTIR spectra of the amide I region of (a) a dried film of FFFF-PEG solution and (b) FFFF-PEG D_2O solutions containing 2.5, 6, 13, 18 wt.% peptide. The peak positions 1 (1673 cm^{-1}) and 2 (1628 cm^{-1}) are associated with secondary structure in the dried film.

observed for the dried film. The splitting of the spectrum, and appearance of a peak due to β-sheet structure suggests a possible critical concentration for self-assembly into β-sheets. This has to be distinguished from initial self-assembly driven by aromatic interactions, which occurs at much lower concentrations as indicated by CD and UV/vis fluorescence experiments. It therefore appears that self-assembly occurs to give quite different structures depending on concentration. At lower concentration self-assembly occurs due to aromatic stacking and hydrophobic interactions into structures without well-defined β-sheets. Defined β-sheets only develop at much higher concentrations. We have previously made similar conclusions for peptide KLVFF [23].

Other peaks were observed in the FTIR spectra. A peak at 1467 cm^{-1} is associated with the amide II band. A broad absorption peak at 2878 cm^{-1}, covers stretching vibration from the benzene rings, CH_2 asymmetric stretching bands and CH_3 symmetric stretching bands. Peaks were also observed in the amide A band at 3283 cm^{-1} and a weak doublet in the amide B region at 3027 and 3060 cm^{-1}.

In summary, FTIR indicates a β-sheet secondary structure in the high concentration solutions and solid samples for FFFF-PEG. CD, UV/visible fluorescence spectra measured at lower concentrations show peaks that result from aromatic stacking interactions. This indicates the formation of aggregates without well-defined β-sheet structure at lower concentration.

To quantitatively determine a critical aggregation concentration (*cac*) resulting from hydrophobic interactions, pyrene fluorescence experiments were performed. This technique is routinely used in the determination of the critical micellar concentration (*cmc*) for amphiphiles [40–43], but it has not to our knowledge been applied for peptide-based systems. Since FFFF-PEG is an amphiphilic hybrid peptide, pyrene fluorescence assays might be a suitable technique to determine the cac.

Fig. 5 shows a series of pyrene fluorescence emission spectra. The results show a weak increase of the fluorescence intensity upon increasing the PEG/peptide concentration with a fixed concentration of pyrene. The increase in fluorescence intensity upon increasing PEG/peptide concentration is enhanced in the range 0.063–0.4 wt.% FFFF-PEG. This increase in intensity reflects the increase of the lifetime of the excited state of pyrene, which is significantly different for different probe surroundings [41]. Pyrene in water has only a very small absorption at 339 nm, which increases substantially upon transfer to a less polar domain [41]. Therefore, the enhancement of the intensity with increasing FFFF-PEG concentration is correlated to the formation of aggregates (fibrils, as shown shortly) and the insertion of the pyrene probe within the hydrophobic cores of those fibres. This idea is supported by the measurement of the I_1/I_3 fraction discussed below.

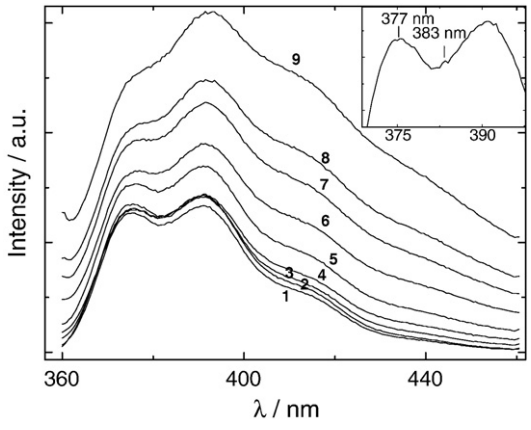

Fig. 5. Fluorescence emission spectra for samples containing 3.6×10^{-6} wt.% pyrene and (1) 0, (2) 6.4×10^{-3}, (3) 2.4×10^{-2}, (4) 4.3×10^{-2}, (5) 6.3×10^{-2}, (6) 0.14, (7) 0.2, (8) 0.27 and (9) 0.4 wt.% FFFF-PEG. The excitation wavelength was 339 nm. The inset shows spectrum 1 (pyrene only) on an enlarged scale.

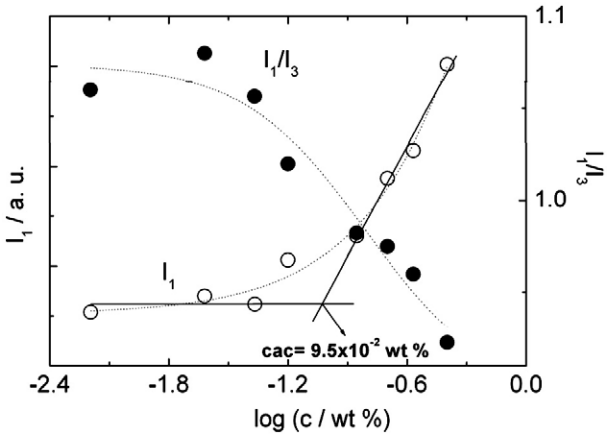

Fig. 6. Dependence of pyrene fluorescence vibronic intensities I_1 and I_1/I_3 as a function of the concentration, using the data plotted in Fig. 4.

The fluorescence intensity of the 0–0 band (λ ~ 373 nm) is denoted I_1, and I_3 (λ ~ 383 nm) is the fluorescence intensity of the third principal vibronic band [44]. The inset in Fig. 5 shows the peaks at 377 nm and 383 nm measured for a sample with 3×10^{-6} wt.% Pyr. Although the peak at 377 nm is well defined, the peak at 383 nm is particularly weak and merges into a shoulder for (0.14–0.4) wt.% FFFF-PEG. Nevertheless, the intensity at 383 nm can still be used to evaluate the ratio I_1/I_3 as a function of FFFF-PEG concentration.

Fig. 6 shows the dependence of I_1 and I_1/I_3 with the concentration, using the spectra in Fig. 5. As discussed above, I_1 increases with increasing concentration due to the change in polarity of the pyrene environment. Below the cac, pyrene is free in the solution and the quantum yield is high, leading to a high I_1/I_3 ratio (Fig. 6). Above the cac, pyrene is selectively sequestered within the fibril core and the I_1/I_3 ratio is reduced. The cac has been determined as illustrated in Fig. 6, from the intersection of linear fits to I_1 data, following the same procedure already used to determine the cmc in the literature [40,41]. Our results indicate a cac value of 0.095 wt.% for FFFF-PEG in water. The CD spectra for a 0.04 wt.% solution (Fig. 1) and the fluorescence spectrum (Fig. 2) were recorded below the cac, which suggests that features in these spectra may reflect local association of aromatic units in pre-aggregates just below the cac, at which point aggregates formed.

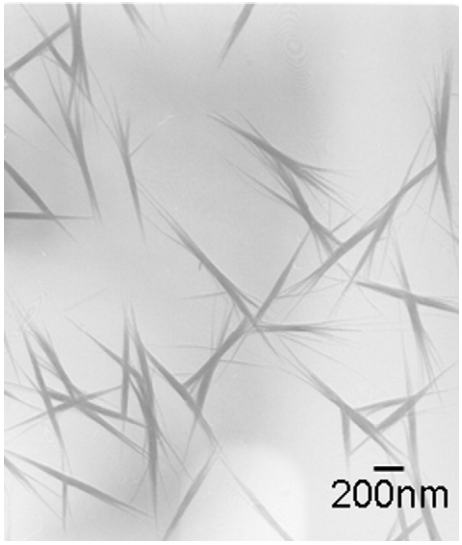

Fig. 7. TEM image of fibrils formed by FFFF-PEG in a film dried from a 5 wt.% aqueous solution.

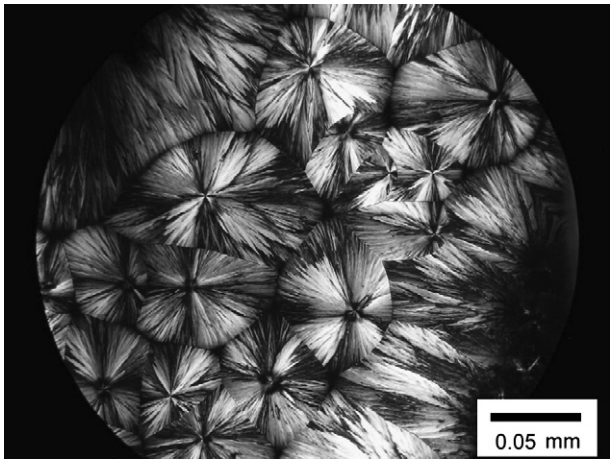

Fig. 8. Polarized optical micrograph showing spherulites resulting from PEG crystallization.

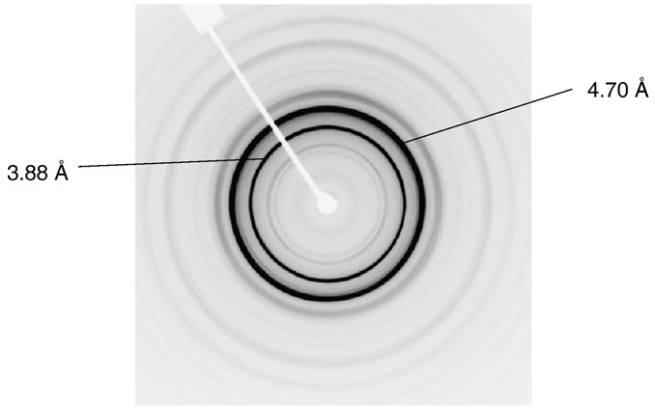

Fig. 10. X-ray fibre diffraction pattern from a dried stalk of FFFF-PEG.

As shown by FTIR, well developed β-sheets are only observed at concentrations much above the cac.

TEM was used to image the self-assembled structures formed by FFFF-PEG above the cac (film dried from 5 wt.% aqueous solution). Fig. 7 shows a representative example of an image obtained. The formation of short rigid fibrils is evident. The "needle-shaped fibrils" are relatively monodisperse in length (887 ± 163) nm and width (32 ± 9) nm. The stiffness and short length of the fibrils may be due to aromatic interactions between, and the high hydrophobicity of, phenylalanine. In particular, the finite length seems to result from a high end cap energy that may reflect the large enthalpic penalty (10.5 kJ mol^{-1}) [45] associated with exposure of phenylalanine to aqueous solution.

4. PEG crystallization in dried films

It was noted that upon drying, PEG crystallization occurred. Evidence for this is provided by polarized optical microscopy, since a characteristic spherulite structure is observed (Fig. 8). These spherulites are similar to those observed for crystallizing polymers such as PEG, and are not of the same form as the amyloid "spherulites" observed previously, which exhibit a "maltese cross" pattern in the polarized optical microscope [46,47]. PEG crystallization, and its effect on peptide β-sheet formation, was further characterized by spectroscopic (FTIR) and X-ray diffraction techniques. We have previously shown that there is a competition between peptide fibrillisation and PEG crystallization in PEG-peptides. In particular, we investigated the series in increasing order of peptide fibrillisation tendency, KLVFF-PEG, AAKLVFF-PEG and FFKLVFF-PEG (all with PEG $M_n = 3000$ g mol^{-1}) [48,49]. In KLVFF-PEG, PEG crystallization strongly disrupted the peptide β-sheet formation, however for FFKLVFF-PEG, PEG crystallization did not occur at the expense of peptide secondary structure formation. AAKLVFF-PEG showed intermediate behaviour. It is interesting to examine the behaviour of FFFF-PEG in this regard.

Fig. 9 presents an FTIR spectrum over a wide range of wavenumbers for a dried film (Fig. 4a shows the amide I region of this spectrum on an expanded scale). The spectrum contains a series of peaks from crystalline poly(ethylene glycol) in the solid state, in addition to peaks from the peptide related to those observed in solution and discussed above. The peaks at 1061, 1111, 1145, 1239, 1266, and a double band at 1335 and 1355 cm^{-1} are all associated with semicrystalline PEG [50].

X-ray diffraction was used to probe PEG crystallization. Fig. 10 shows an X-ray diffraction pattern obtained for a dried stalk of the sample. Other images were obtained with longer sample-detector distances in order to resolve large *d* spacing peaks at small angles. The specimen was not highly aligned, but nonetheless a series of peaks are evident. Many of the reflections can be indexed based on the monoclinic unit cell of PEG (Table 1) [51]. There are additional reflections with longer *d* spacings that result from the FFFF β-sheet structure. It has also to be considered that there is likely to be overlap of some reflections from the β-sheet structure and those from PEG, in particular the main 4.7 Å peak from the backbone spacing in the β-sheet is probably superposed on the most intense 120 peak from crystalline PEG [49]. The combination of peaks from the β-sheet stacking of the peptide (*d* spacing too large to be indexed using the PEG unit cell) and those from crystalline PEG, indicate that the β-sheet structure is not totally destroyed by PEG crystallization, although the peaks from the β-sheet structure are rather weak pointing to the predominant effect of crystallization.

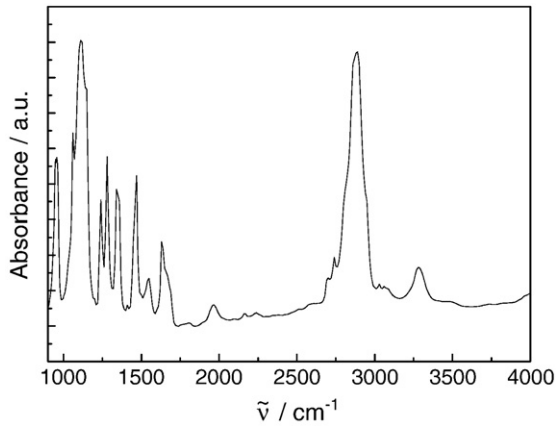

Fig. 9. FTIR spectrum for dried film.

Table 1
X-ray diffraction: observed *d* spacings, and calculated *d* spacings (with indexation and structure factor F_{hkl}) for PEG.

Reflection	*d*/Å (observed)	*d*/Å (calculated)	F_{hkl} (calculated)
	27.9	From peptide	
	12.0 (broad)	From peptide	
	6.81	From peptide?	
021	5.98	6.03/5.86	24/31
120	4.70	4.63	197
112	3.88	3.86	37
032/$\bar{1}$32($\bar{2}$12)	3.82	3.81/3.78	194/171 (148)
123	2.94	2.94	49
$\bar{2}$31/043	2.78	2.80/2.78	27/41
	2.53	Many peaks	
	2.31	Many peaks	

5. Summary

Despite the remarkably short peptide sequence, the peptide block copolymer FFFF-PEG5000 shows amphiphilic self-assembly in aqueous solution and nanostructure formation in the solid state. Self-assembly due to hydrophobic interactions of aromatic phenylalanine residues occurs at low concentration in aqueous solution, well-defined β-sheets developing at higher concentration. PEGylation does not influence the uptake of the thioflavin T fluorophore, and the peptide-PEG conjugate itself shows an interesting fluorescence feature. Drying causes PEG to crystallize, leading to macroscopic spherulite formation. These spherulites result from the PEG crystallization and are not amyloid aggregate spherulites. PEG crystallization does not however completely disrupt peptide β-sheet formation, as shown by FTIR and X-ray diffraction.

PEG with $M_n = 4850$ g mol^{-1} has 110 repeats of ethylene oxide. This leads to a "surfactant" with a much longer PEG chain length than for conventional non-ionic surfactants (eg. $C_{12}EO_6$, where C indicates methylene and EO ethylene oxide). Our study concerns a molecule in the "polymeric limit". We have also examined the self-assembly of FFFF-PEG3000, with very similar results to those presented here (cryo-TEM confirmed the formation of short needle-like fibrils). However, FF-PEG3000 did not show self-assembly properties (i.e. β-sheet peaks were not observed in the amide I region in the FTIR spectrum, and fibrils were not observed via electron microscopy). This indicates that sufficient hydrophile/liphophile balance (HLB) in terms of numbers of phenylalanine repeats with respect to PEG chain length is required to observe self-assembly properties. The concept of using short peptide end groups offers the scope for novel methods to tailor polymer self-assembly, and could be developed to exploit more specific functionalities of short peptide sequences.

Acknowledgements

We would like to acknowledge Prof. J. Gibbins (School of Biological Sciences, Univ. of Reading) for providing the facilities for the fluorescence experiments, Dr Rebecca Green (Dept. of Pharmacy, Univ. of Reading) for access to the FTIR instrument, Dr Peter Harris (Centre for Advanced Microscopy, University of Reading) for help with TEM experiments, Dr. Louise C. Serpell (Dept. of Biochemistry, Univ. of Sussex) for providing a copy of the software CLEARER and Mr. Nick Spencer (Biocentre, Univ. of Reading) for assistance with XRD experiments.

References

[1] B. Jönsson, B. Lindman, K. Holmberg, B. Kronberg, Surfactants and Polymer in Aqueous Solution, John Wiley, Chichester, 1998.
[2] I.W. Hamley, Introduction to Soft Matter, Revised Edition, Wiley, Chichester, 2007.
[3] H.-A. Klok, J. Polym. Sci., A, Polym. Chem. 43 (2004) 1.
[4] H.G. Börner, H. Schlaad, Soft Matter 3 (2007) 394.
[5] D.W.P.M. Löwik, L. Ayres, J.M. Smeenk, J.C.M. van Hest, Adv. Polym. Sci. 202 (2006) 19.
[6] J.D. Hartgerink, E. Beniash, S.I. Stupp, Science 294 (2001) 1684.
[7] J.D. Hartgerink, E. Beniash, S.I. Stupp, Proc. Natl. Acad. Sci. U. S. A. 99 (2002) 5133.
[8] K.L. Niece, J.D. Hartgerink, J.J.J.M. Donners, S.I. Stupp, J. Am. Chem. Soc. 125 (2003) 7146.
[9] S. Santoso, W. Hwang, H. Hartman, S. Zhang, Nano Lett. 2 (2002) 687.
[10] X. Zhao, S. Zhang, Trends Biotech. 22 (2004) 470.
[11] D.W.P.M. Löwik, J. Garcia-Hartjes, J.T. Meijer, J.C.M. van Hest, Langmuir 21 (2005) 524.
[12] T.S. Burkoth, T.L.S. Benzinger, D.N.M. Jones, K. Hallenga, S.C. Meredith, D.G. Lynn, J. Am. Chem. Soc. 120 (1998) 7655.
[13] T.S. Burkoth, T.L.S. Benzinger, V. Urban, D.G. Lynn, S.C. Meredith, P. Thiyagarajan, J. Am. Chem. Soc. 121 (1999) 7429.
[14] H.-A. Klok, G.W.M. Vandermeulen, H. Nuhn, A. Rösler, I.W. Hamley, V. Castelletto, H. Xu, S. Sheiko, Faraday Discuss. 128 (2005) 29.
[15] I.W. Hamley, I.A. Ansari, V. Castelletto, H. Nuhn, A. Rösler, H.-A. Klok, Biomacromolecules 6 (2005) 1310.
[16] D. Eckhardt, M. Groenewolt, E. Krause, H.G. Börner, Chem. Commun. 2005 (2005) 2814.
[17] I.W. Hamley, M.J. Krysmann, V. Castelletto, L. Noirez, Adv. Mater. 20 (2008) 4394.
[18] S. Vauthey, S. Santoso, H. Gong, N. Watson, S. Zhang, Proc. Natl. Acad. Sci. U. S. A. 99 (2002) 5355.
[19] D.J. Adams, K. Holtzmann, C. Schneider, M.F. Butler, Langmuir 23 (2007) 12729.
[20] H.G. Börner, B. Smarsly, J. Hentschel, A. Rank, R. Schubert, Y. Geng, D.E. Discher, T. Hellweg, A. Brandt, Macromolecules 41 (2008) 1430.
[21] J.T. Meijer, M. Roeters, V. Viola, D. Lowik, G. Vriend, J.C.M. van Hest, Langmuir 23 (2007) 2058.
[22] I.W. Hamley, Angew. Chem., Int. Ed. Engl. 46 (2007) 8128.
[23] M.J. Krysmann, V. Castelletto, A. Kelarakis, I.W. Hamley, R.A. Hule, D.J. Pochan, Biochemistry 47 (2008) 4597.
[24] M.J. Krysmann, V. Castelletto, I.W. Hamley, Soft Matter 3 (2007) 1401.
[25] I.W. Hamley, M.J. Krysmann, V. Castelletto, A. Kelarakis, L. Noirez, R.A. Hule, D. Pochan, Chem. Eur. J. 14 (2008) 11369.
[26] I.W. Hamley, M.J. Krysmann, G.E. Newby, V. Castelletto, L. Noirez, Phys. Rev., E 57 (2008) 062901.
[27] M. Reches, E. Gazit, Science 300 (2003) 625.
[28] R. Azriel, E. Gazit, J. Biol. Chem. 276 (2001) 34156.
[29] M. Reches, Y. Porat, E. Gazit, J. Biol. Chem. 277 (2002) 35475.
[30] V. Jayawarna, M. Ali, T.A. Jowitt, A.F. Miller, A. Saiani, J.E. Gough, R.V. Ulijn, Adv. Mater. 18 (2006) 611.
[31] A.M. Smith, R.J. Williams, C. Tang, P. Coppo, R.F. Collins, M.L. Turner, A. Saiani, R.V. Ulijn, Adv. Mater. (Weinheim, Fed. Repub. Ger.) 20 (2008) 37.
[32] F.W.J. Teale, G. Weber, Biochem. J. 65 (1957) 476.
[33] H. LeVine, Protein Sci. 2 (1993) 404.
[34] M.R. Nilsson, Methods 34 (2004) 151.
[35] E. Lee, Z. Huang, J.-H. Ryu, M. Lee, Chem. Eur. J. 14 (2008) 6957.
[36] B. Stuart, Biological Applications of Infrared Spectroscopy, Wiley, Chichester, 1997.
[37] J.T. Pelton, L.R. McLean, Anal. Biochem. 277 (2000) 167.
[38] W.K. Surewicz, H.H. Mantsch, Biochim. Biophys. Acta 952 (1988) 115.
[39] M. Jackson, H.H. Mantsch, Crit. Rev. Biochem. Mol. Biol. 30 (1995) 95.
[40] M. Johnsson, P. Hansson, K. Edwards, J. Phys. Chem. B 105 (2001) 8420.
[41] M. Wilhelm, C.-L. Zhao, Y. Wang, R. Xu, M.A. Winnik, J.-L. Mura, G. Riess, M.D. Croucher, Macromolecules 24 (1991) 1033.
[42] I. Astafieva, X.F. Zhong, A. Eisenberg, Macromolecules 26 (1993) 7339.
[43] I. Astafieva, K. Khogaz, A. Eisenberg, Macromolecules 28 (1995) 7127.
[44] M. Johnsson, M. Silvander, G. Karlsson, K. Edwards, Langmuir 15 (1999) 6314.
[45] T.E. Creighton, Proteins. Structures and Molecular Properties, W.H.Freeman, New York, 1993.
[46] M.R.H. Krebs, C.E. MacPhee, A.F. Miller, L.E. Dunlop, C.M. Dobson, A.M. Donald, Proc. Natl. Acad. Sci. U. S. A. 101 (2004) 14420.
[47] M.R.H. Krebs, E.H.C. Bromley, S.S. Rogers, A.M. Donald, Biophys. J. 88 (2005) 2013.
[48] M.J. Krysmann, I.W. Hamley, S.S. Funari, E. Canetta, Macromol. Chem. Phys. 209 (2008) 883.
[49] I.W. Hamley, M.J. Krysmann, Langmuir 24 (2008) 8210.
[50] Y. Zheng, M.L. Bruening, G.L. Baker, Macromolecules 40 (2007) 8212.
[51] Y. Takahashi, H. Tadokoro, Macromolecules 6 (1973) 672.